Catalytic Decomposition of $H_2O(D_2O)$ on a Heated Ir Filament to Produce O and OH(OD) Radicals

Hironobu Umemoto* and Hiroki Kusanagi

Faculty of Engineering, Shizuoka University, Johoku, Naka, Hamamatsu, Shizuoka 432-8561, Japan

Abstract: Production of O atoms, H(D) atoms, and OH(OD) radicals was confirmed in the catalytic decomposition of $H_2O(D_2O)$ on a heated Ir filament by laser spectroscopic techniques, such as vacuum-ultraviolet laser-induced fluorescence. The highest steady-state OH density achieved was 2×10^{11} cm^{-3}. The filament temperature dependences of the radical densities were not Arrhenius-type, in contrast to the results on the decomposition of H_2 and O_2. Especially, OH(OD) density decreased with the increase in the filament temperature over 2100 K. The decomposition process changes from the production of H+OH(D+OD) to that of 2H+O(2D+O) with the increase in the catalysis temperature. This change in the exit channel could not be reproduced by model calculations using the CHEMKIN software package when Arrhenius-type temperature dependences were assumed for the elementary-step rate constants on surfaces. It is necessary to assume that the desorption energy of OH(OD) is surface coverage dependent.

---

* Address correspondence to this author at the Faculty of Engineering, Shizuoka University, Johoku, Naka, Hamamatsu, Shizuoka 432-8561, Japan; Tel: +81-53-478-1275; Fax: +81-53-478-1275; E-mail: thumemo(at)ipc.shizuoka.ac.jp

Running title: Catalytic Decomposition of $H_2O(D_2O)$

Introduction

Catalytic chemical vapor deposition (Cat-CVD), often called hot-wire CVD, is one of the promising techniques for the preparation of high-quality thin films [1, 2]. In this technique, radical species are produced from material gases on heated metal surfaces without co-producing ionic or metastable excited species. In order to make clear the decomposition and ejection mechanisms, many studies have been carried out to identify the radical species produced [3-16]. Although it has been rather difficult to produce oxidizing radicals, we have recently shown that atomic oxygen can be produced efficiently by the catalytic decomposition of O_2, NO, N_2O, and NO_2 on a heated Ir filament [7, 8]. It was also shown that Ir is not oxidized by these species when heated up to 2350 K and that metal contamination on the deposited films is minor. Among these oxidizing species, the O-atom density in the gas phase was the highest when O_2 was used as a source gas. The catalyst temperature dependence of the density was Arrhenius-type and the O-atom density could be increased up to 2×10^{12} cm^{-3} [7].

Molecular oxygen has already been used as one of the source gases to prepare SiO_xN_y thin films [17]. Since SiO_xN_y is less dense and more flexible compared to SiN_x, that can be used as an interlayer to cover the microslits formed in SiN_x films, which can be used as passivation films for organic light emitting diodes. The problem is that O_2 is reactive to SiH_4, one of the most widely used source gases of silicon. The situation is similar when N_2O is used as a source gas. H_2O is another potential volatile source of O atoms in the preparation of SiO_xN_y films. The reaction between SiH_4 and H_2O in the gas phase is slow at moderate temperatures. The production of SiH_3OH+H_2 is exothermic, but the activation energy has been calculated to be more than 200 kJ mol^{-1} [18].

In the present work, the absolute densities of O atoms, H(D) atoms, and OH(OD) radicals produced by the catalytic decomposition of $H_2O(D_2O)$ on a heated Ir filament were evaluated under various conditions by laser spectroscopic techniques. Model calculations using the CHEMKIN software package were also carried out.

Materials and Methodology

The experimental apparatus and the procedure were similar to those described elsewhere [6-8]. A cylindrical reaction chamber, 10 cm in internal diameter, made of stainless steel was used. An Ir wire (Tanaka Precious Metals, 30 cm in length and 0.50 mm in diameter, 99.9%) was resistively heated by using a DC power supply. Neat $H_2O(D_2O)$ was used without dilution otherwise stated. The flow rate was controlled by using a mass flow controller (STEC, SEC-8440LS). The typical flow rate was 1.5 sccm and the pressure was 0.8 Pa. Another mass flow controller (STEC, SEC-7320M) was used in the O_2 added systems. The catalyst temperature was estimated from the relationship between the electric resistivity and the temperature [19].

Atomic hydrogen produced on the heated Ir catalyst was detected by employing three techniques; vacuum-ultraviolet laser-induced fluorescence (vuv LIF) at 121.6 nm, vacuum-ultraviolet

laser absorption at 121.6 nm, and two-photon laser-induced fluorescence at 205.1 nm. By employing these techniques, it is possible to determine the absolute densities under wide conditions [6]. Atomic deuterium was detected similarly. Atomic oxygen was detected by a vuv LIF technique at 130.2 nm. The absolute densities were evaluated by comparing the signal intensities with those in pure O_2 systems, where the absolute densities have been determined by a laser absorption technique [7]. OH(OD) radicals were detected by employing an LIF technique in the ultraviolet region. The absolute densities of OH were evaluated by comparing the time integrated LIF intensity for the $P_1(N''=2, J''=3/2)$ transition at 308.6 nm under saturated conditions with the intensity of Rayleigh scattering caused by Ar [6]. The absolute OD densities were evaluated from the LIF intensity of the $P_1(N''=4, J''=7/2)$ transition at 308.2 nm. The distance between the catalyst and the radical detection zone was 9 cm. Mass spectrometric analysis was also carried out to estimate the consumption efficiency of D_2O, since D_2O^+ signals can be measured with less influence of background signals.

O_2 (Takachiho, 99.99%) and Kr (Nihon Sanso, 99.995%) were used from cylinders without further purification. H_2O was used after distillation and degassing in vacuum. D_2O was the product of Aldrich (nominal isotopic purity 99.9%).

Results

O atoms, H(D) atoms, and OH(OD) radicals were identified by laser spectroscopic techniques. Fig. (1) shows the observed and simulated LIF spectra of OD produced from D_2O. In the simulation, spectroscopic data obtained by Clyne *et al.* were employed [20]. The rotational transition probabilities were assumed to be the same as those of $OH(A^2\Sigma^+\text{-}X^2\Pi)$ transitions [21, 22]. The LIF spectrum of OH produced from H_2O was very similar to those reported previously for the catalytic decomposition of H_2/O_2 mixtures [6, 8]. The rotational distributions of OH and OD radicals could be fitted by a Boltzmann distribution at 350 K. This result shows that the rotational relaxation is rapid even when the total pressure is as low as 0.8 Pa. Vibrationally excited OH(OD) radicals were not identified. No H/D isotope effects could be observed not only in the state distributions but also in the absolute densities. This suggests that quantum effects, such as tunneling, cannot be important. If tunneling plays important roles, the yield of H atoms must be larger than that of D atoms. All the radical species increased with the increase in the $H_2O(D_2O)$ flow rate, as is shown in Fig. (2), although the increase is not exactly linear. As for OH, we have confirmed the increase against the flow rate up to 3.00 sccm (1.6 Pa in pressure) and found that the density can be as high as 7.0×10^{10} cm^{-3}.

It should be noted that the catalysis temperature dependences of the radical densities were not Arrhenius-type for all radical species as are shown in Fig. (3). Especially, the OH(OD) density showed a maximum around 2100 K and then decreased. The H-atom densities were evaluated by vuv LIF (below 1920 K), vuv laser absorption (at 2060 K), and two-photon LIF (over 2150 K) techniques. The absolute densities were determined by comparing the LIF intensities with that in pure H_2 systems except

at 2060 K. At 2060 K, the absolute density was determined from the transmittance directly. The absolute O-atom densities were determined by comparing the LIF signal intensities with those observed in pure O_2 systems [7]. When the atomic densities are high, vuv LIF signals may be reduced because of the absorption of the vuv laser radiation by atomic species. Such effects were corrected in the plots in Figs. (2) and (3). The correction factors were less than 10% both for H and O atoms.

The OH density could be increased by the addition of O_2. When 1.00 sccm of O_2 was added to 1.50 sccm of H_2O, the OH density increased from 3.7×10^{10} to 1.6×10^{11} cm^{-3} when the catalyst temperature was 2100 K. This value is much larger than those observed in the decomposition of H_2/O_2 mixtures [6, 8]. The decrease in the OH density with the increase in the catalyst temperature over 2100 K could also be observed in the presence of O_2, but the decrease was more gradual compared to that in the absence of O_2. In the presence of O_2, H atoms must have been converted to OH radicals.

Mass-spectrometric measurements were carried out for D_2O to estimate the consumption efficiency, since much less background signals are expected compared to H_2O. The decrease in the D_2O^+ signals when the catalysis was heated was found to be minor. This may partly be ascribed to the reproduction of D_2O molecules from radical species on chamber walls. The D_2^+ and O_2^+ signals were less than 10% of that of D_2O^+, under any conditions, and the consumption efficiency of D_2O is estimated to be less than 20%. No change in electric resistivity was observed when the filament was kept at 2350 K in the presence of 1.6 Pa of water vapor, showing that the oxidation of the filament is not taking place.

Discussion

The decrease in the OH densities over 2100 K suggests that H_2O is decomposed completely to 2H+O at high catalyst temperatures. At low temperatures, the main exit channel is H+OH and the production efficiency increases with the temperature. On the other hand, at high temperatures, the complete decomposition to produce 2H+O becomes more efficient and the production of OH is suppressed. This idea is supported by the result that the [H]/[O] density ratio is around 2 at high catalyst temperatures. A similar complete decomposition mechanism has been proposed for SiH_4 when the W catalyst temperature is higher than 2000 K [23, 24]. In this case, SiH_2 and SiH_3 densities decreased with the increase in the catalysis temperature [23]. The decrease in the OH densities may not be ascribed to the increase in the removal rate of OH on chamber walls, since the change in the OH density was immediate when the catalyst temperature was changed. The chamber wall temperature may not change so rapidly.

Model calculations using the CHEMKIN software package were carried out to make clear why the exit channel changes from H+OH to 2H+O. In the CHEMKIN simulation, a plug-flow reactor model with one inlet and one outlet was employed. It was assumed that the temperature in the reactor is uniform and that H_2O is decomposed on hot Ir walls. Such a reactor model is different from the present experimental setup and quantitative discussion may not be valid. However, semi-quantitative

discussion may still be possible, since CHEMKIN software has been applied successfully to many chemical systems [25, 26]. The site density of Ir was calculated from its density and atomic weight to be 2.8×10^{-9} mol cm^{-2}. Gas-phase reactions may be ignored since H_2O molecules are unreactive to radical species at moderate temperatures. Thermal decomposition of H_2O in the gas phase is slow [27]. Reactions between radical species in the gas phase can be ignored because of their low densities. It was easy to reproduce the decrease in the gas-phase OH density at high Ir temperatures under the conditions that H_2O is depleted. However, the depletion of D_2O was not confirmed by the present quadrupole mass spectrometric measurements.

The present result of the non-Arrhenius behavior of the OH density, including the presence of an optimum temperature to produce OH radicals, can be reproduced under the conditions without H_2O depletion by assuming the following elementary steps on catalysis surfaces, if no restrictions are imposed to the rate parameters:

$H_2O + Ir\_$	$\rightarrow$	$H_2O\_$	(1)
$H_2O\_$	$\rightarrow$	$H_2O + Ir\_$	(2)
$H_2O\_ + Ir\_$	$\rightarrow$	$OH\_ + H\_$	(3)
$OH\_ + Ir\_$	$\rightarrow$	$O\_ + H\_$	(4)
$OH\_$	$\rightarrow$	$OH + Ir\_$	(5)
$H\_$	$\rightarrow$	$H + Ir\_$	(6)
$O\_$	$\rightarrow$	$O + Ir\_$	(7)

Here, _ represents adsorbed species or a vacant site on Ir. The problem is that unreasonably large or small preexponential factors have to be assumed to reproduce the temperature dependence of the OH density. At high catalyst temperatures, the OH production must be minor compared to O- and H-atom production processes. In other words, in order to reproduce the present experimental results, both the preexponential factor and the activation energy for reaction (4) must be large, while those for reaction (5) must be small. In general, the preexponential factor for the decomposition processes on surfaces, such as reaction (4), should be in the order of 10^{22} cm^2 mol^{-1} s^{-1}, while that for desorption processes from surfaces, such as reaction (5), should be around 10^{13} s^{-1} [28, 29]. The present results could not be reproduced by simulations when these typical parameters were assumed. For example, when the preexponential factor for reaction (5) was assumed to be 1×10^{13} s^{-1}, it was necessary to assume the preexponential factor for reaction (4) to be 1×10^{30} cm^2 mol^{-1} s^{-1} to reproduce the temperature dependence of the OH density. This preexponential factor for reaction (4) is too large. The non-Arrhenius behavior of the OH density could not be reproduced by including some surface reactions, such as $H+OH\_ \rightarrow H_2O\_$ and $OH\_+OH\_ \rightarrow H_2O\_+O\_$, either.

The concept of “coverage dependent desorption energy” is useful to explain the non-Arrhenius temperature dependence of the OH density. In general, activation energies depend on the surface coverage [28]. For example, the desorption energy of OH radicals from heated Pd surfaces

decrease with the increase in the surface coverage [30, 31]. Of course, the surface coverage decreases with the increase in the catalysis temperature. If we assume that the activation energy for OH desorption, reaction (5), depends linearly on the surface coverage, θ, according to 375-154θ kJ mol^{-1}, that increases from 251 to 341 kJ mol^{-1} when the catalyst temperature increases from 1700 to 2400 K, and the present experimental results can be reproduced, at least semi-quantitatively. Fig. (4) illustrates the simulated results. In this simulation, the preexponential factors for desorption processes, reactions (2), (5), (6), and (7), were all assumed to be 1×10^{12} s^{-1}, while those for reactions (3) and (4) were assumed to be 5×10^{22} cm^2 mol^{-1} s^{-1}. Just for simplicity, the activation energies for reactions other than reaction (5) were assumed to be coverage independent and between 100 and 380 kJ mol^{-1}. The curvature in the plot for H atoms is not reproduced well in the simulation, but this may also be caused by the coverage dependence of the H-atom desorption energy and some Langmuir-Hinshelwood reactions on Ir surfaces, such as H_+OH_ $\rightarrow$ H_2O_+Ir_. The slight curvature observed for O atoms in Fig. (4) must be caused by the competition between reactions (2) and (3). The increase in OH densities in the presence of O_2 is consistent with this model. The surface coverage should be higher in the presence of O_2, and the desorption rate of OH should be larger. It should be noted that a linear Arrhenius plot has been observed in the decomposition of O_2 on heated Ir surfaces, although the residence time of atomic oxygen is expected to be long [7]. This can be accounted for by considering that Ir surfaces are completely covered with O atoms at all temperatures in the presence of 0.8 Pa of pure O_2. The decomposition of O_2 may principally take place on the adsorbed layer of O atoms.

In the catalytic decomposition of O_2 on heated Ir, the O-atom density showed saturation against the O_2 flow rate. This has been explained by the shortage of the active sites on catalysis surfaces [7]. Ir surfaces may be covered with O atoms to suppress the decomposition of O_2. Similar slight upward curvature can be observed in the H_2O flow rate dependence of the O-atom density. On the other hand, the OH density shows downward curvature. This can also be explained by the coverage dependence of the desorption energy. At low pressures, the coverage is low, the activation energy for OH desorption is large, and the production rate of OH is low. At high pressures, the coverage is high and the production rate of OH can be high.

The OH-radical density obtained in the present system is higher than those obtained in the catalytic decomposition of H_2/O_2 mixed systems [6, 8]. However, that is less than those reported in plasma processes [32-36]. For example, the OH density can be as high as 3×10^{15} cm^{-3} after a pulsed discharge of a mixture of H_2O and Ar [36]. However, in pulsed discharges, the OH density decays within 0.1 ms or less. Since the repetition rate of discharges is usually less than 10 Hz, the time-averaged density should be in the order of 10^{12} cm^{-3} or less. In addition, in corona discharges, the discharge volume cannot be large. It is, of course, possible to produce OH radicals in DC discharges, but in such cases, the OH density is much less than those observed in pulsed discharges, in the order of 10^{11} cm^{-3} [37], which is comparable to that observed in the present system. The merit in catalytic

decomposition is that no ionic or metastable excited species are produced. In addition, radicals can easily be produced in a large volume. The OH density may still be increased just by increasing the H_2O pressure, since no saturation has been observed up to 1.6 Pa.

Conclusions

Catalytic decomposition processes of $H_2O(D_2O)$ on a heated Ir filament were examined by employing laser spectroscopic techniques. Ir was not oxidized even when it was heated up to 2350 K in the presence of 1.6 Pa of water vapor. The exit channel changes from the production of OH(OD)+H(D) to that of 2H(2D)+O with the increase in the catalyst temperature and the radical densities showed non-Arrhenius temperature dependences. It is necessary to assume a coverage-dependent desorption energy for OH(OD) to make the simulations to agree with the experimental results. The maximum density of OH in the gas-phase was 7.0×10^{10} cm^{-3} when the H_2O pressure was 1.6 Pa. This OH density is comparable to that observed in DC discharge plasma. The OH density may still be increased just by increasing the H_2O pressure. In addition, the OH density could be increased by a factor of 4 by the introduction of O_2.

Acknowledgement

This work was partially funded by the Grant-in-Aid for Science Research (No. 19550015) from the Japan Society for the Promotion of Science.

REFERENCES

[1] Matsumura H. Formation of Silicon-based thin films prepared by catalytic chemical vapor deposition (Cat-CVD) method. Jpn J Appl Phys 1998; 37: 3175-87.

[2] Matsumura H, Ohdaira K. New application of Cat-CVD technology and recent status of industrial implementation. Thin Solid Films 2009; 517: 3420-3.

[3] Nozaki Y, Kongo K, Miyazaki T, *et al*. Identification of Si and SiH in catalytic chemical vapor deposition of SiH_4 by laser induced fluorescence spectroscopy. J Appl Phys 2000; 88: 5437-43.

[4] Umemoto H, Ohara K, Morita D, Nozaki Y, Masuda A, Matsumura H. Direct detection of atomic hydrogen in the catalytic chemical vapor deposition of the SiH_4/H_2 system. J Appl Phys 2002; 91: 1650-6.

[5] Umemoto H, Ohara K, Morita D, *et al*. Radical species formed by the catalytic decomposition of NH_3 on heated W surfaces. Jpn J Appl Phys 2003; 42: 5315-21.

[6] Umemoto H, Moridera M. Production and detection of reducing and oxidizing radicals in the catalytic decomposition of H_2/O_2 mixtures on heated tungsten surfaces. J Appl Phys 2008; 103: 034905.

[7] Umemoto H, Kusanagi H. Catalytic decomposition of O_2, NO, N_2O and NO_2 on a heated Ir filament to produce atomic oxygen. J Phys D: Appl Phys 2008; 41: 225505.

[8] Umemoto H, Kusanagi H, Nishimura K, Ushijima M. Detection of radical species produced by catalytic decomposition of H_2, O_2 and their mixtures on heated Ir surfaces. Thin Solid Films 2009; 517: 3446-8.

[9] Duan HL, Zaharias GA, Bent SF. Detecting reactive species in hot wire chemical vapor deposition. Current Opinion Solid State Mater Sci 2002; 6: 471-7.

[10] Zheng W, Gallagher A. Hydrogen dissociation on high-temperature tungsten. Surf Sci 2006; 600: 2207-13.

[11] Zheng W, Gallagher A. Radical species involved in hotwire (catalytic) deposition of hydrogenated amorphous silicon. Thin Solid Films 2008; 516: 929-39.

[12] Tonokura K, Koshi M. Reaction kinetics in silicon chemical vapor deposition. Current Opinion Solid State Mater Sci 2002; 6: 479-85.

[13] Redman SA, Chung C, Rosser KN, Ashfold MNR. Resonance enhanced multiphoton ionisation probing of H atoms in a hot filament chemical vapour deposition reactor. Phys Chem Chem Phys 1999; 1: 1415-24.

[14] Comerford DW, Cheesman A, Carpenter TPF, *et al*. Experimental and modeling studies of B atom number density distributions in hot filament activated B_2H_6/H_2 and $B_2H_6/CH_4/H_2$ gas mixtures. J Phys Chem A 2006; 110: 2868-75.

[15] Shi YJ, Eustergerling BD, Li XM. Mass spectrometric study of gas-phase chemistry in the hot-wire CVD processes of SiH_4/NH_3 mixture. Thin Solid Films 2008; 516: 506-10.

[16] Tong L, Shi YJ. A mechanistic study of gas-phase reactions with 1,1,3,3-tetramethyl-1,3-disilacyclobutane in the hot-wire chemical vapor deposition process. Thin Solid Films 2009; 517: 3461-5.

[17] Ogawa Y, Ohdaira K, Oyaidu T, Matsumura H. Protection of organic light-emitting diodes over 50 000 hours by Cat-CVD SiN_x/SiO_xN_y stacked thin films. Thin Solid Films 2008; 516: 611-4.

[18] Hu SW, Wang Y, Wang XY, Chu TW, Liu XQ. Gas-phase reactions between silane and water: A theoretical study. J Phys Chem A 2004; 108: 1448-59.

[19] Wimber RT, Halvorson JJ. Electrical resistivity of iridium at high temperatures. J Mater 1972; 7: 564-7.

[20] Clyne MAA, Coxon JA, Fat ARW. The $A^2\Sigma^+$-$X^2\Pi_i$ electronic band system of the OD free radical : Spectroscopic data for the 0-0 sequence, and rotational term values for $A^2\Sigma^+$ and $X^2\Pi_i$. J Mol Spectrosc 1973; 46: 146-70.

[21] Dimpfl WL, Kinsey JL. Radiative lifetimes of OH($A^2\Sigma$) and Einstein coefficients for the A-X system of OH and OD. J Quant Spectrosc Rad Trans. 1979; 21: 233-41.

[22] Chidsey IL, Crosley DR. Calculated rotational transition probabilities for the $A-X$ system of OH. J Quant Spectrosc Rad Trans 1980; 23; 187-99.

[23] Tange S, Inoue K, Tonokura K, Koshi M. Catalytic decomposition of SiH_4 on a hot filament. Thin Solid Films 2001; 395: 42-6.

[24] Duan HL, Bent SF. The influence of filament material on radical production in hot wire chemical vapor deposition of a-Si:H. Thin Solid Films 2005; 485: 126-34.

[25] Nakamura S, Matsumoto K, Susa A, Koshi M. Reaction mechanism of silicon Cat-CVD. J Non-Cryst Solids 2006; 352: 919-24.

[26] Nakamura S, Koshi M. Elementary processes in silicon hot wire CVD. Thin Solid Films 2006; 501: 26-30.

[27] Baulch DL, Cobos CJ, Cox RA, *et al*. Evaluated kinetic data for combustion modeling. J Phys Chem Ref Data 1992; 21: 411-734.

[28] Zhdanov VP, Pavlíček J, Knor Z. Preexponential factors for elementary surface processes. Catal Rev 1988; 30: 501-17.

[29] Deutschmann O, Schmidt R, Behrendt F, Warnatz J. Numerical modeling of catalytic ignition. Twenty-Sixth Symp (Inter) Combust 1996; 26: 1747-54.

[30] Johansson Å, Försth M, Rosén A. A comparative study of high-temperature water formation and OH desorption on polycrystalline palladium and platinum catalysts. Surf Sci 2003; 529: 247-66.

[31] Andrae JCG, Johansson Å, Björnbom P, Rosén A. OH desorption energies for a palladium catalyst characterised by kinetic modelling and laser-induced fluorescence. Surf Sci 2004; 563: 145 -58.

[32] Hibert C, Gaurand I, Motret O, Pouvesle JM. [OH(X)] measurements by resonant absorption spectroscopy in a pulsed dielectric barrier discharge. J Appl Phys 1999; 85: 7070-5.

[33] Ono R, Oda T. Dynamic and density estimation of hydroxyl radicals in a pulsed corona discharge. J Phys D: Appl Phys 2002; 35: 2133-8.

[34] Ono R, Oda T. Dynamics of ozone and OH radicals generated by pulsed corona discharge in humid-air flow reactor measured by laser spectroscopy. J Appl Phys 2003; 93: 5876-82.

[35] Ono R, Oda T. Measurements of gas temperature and OH density in the afterglow of pulsed positive corona discharge. J Phys D: Appl Phys 2008; 41: 035204.

[36] Tochikubo F, Uchida S, Watanabe T. Study on decay characteristics of OH radical density in pulsed discharge in Ar/H_2O. Jpn J Appl Phys 2004; 43: 315-20.

[37] Ito K, Hagiwara K, Nakaura H, Tanaka H, Onda K. Radical density measurement at low-pressure discharge denitrification by appearance mass spectrometry. Jpn J Appl Phys 2001; 40: 1472-6.

Figure Captions

Fig. (1). Experimental (upper) and simulated (lower) spectra of OD in a pure D_2O system. The flow rate and the pressure were 1.50 sccm and 0.8 Pa, respectively. The catalyst temperature was 2100 K. The assignments are shown for the P_1, Q_1, P_2, Q_2, and R_2 branches of the (0,0) band. The numbers are the total angular momentum quantum numbers exclusive of nuclear and electron spin. The rotational temperature was assumed to be 350 K in the simulation.

Fig. (2). H-atom (Δ), O-atom(○), and OH-radical(■) densities as a function of H_2O flow rate. The catalyst temperature was 2100 K.

Fig. (3). H-atom (▲, ▼, Δ), O-atom(○), and OH-radical(■) densities as a function of the reciprocal of catalyst temperature in a pure H_2O system. Results for H atoms obtained by a two-photon LIF technique are represented by ▲, that by laser absorption is represented by ▼, and those by one-photon LIF are represented by Δ. The flow rate and the pressure were 1.50 sccm and 0.8 Pa, respectively.

Fig. (4). H-atom (Δ), O-atom (○), and OH-radical (■) densities calculated by the CHEMKIN software package. The preexponential factors for reactions (4) and (5) were assumed to be 5×10^{21} cm^2 mol^{-1} s^{-1} and 1×10^{12} s^{-1}, respectively. The activation energy for reaction (4) was assumed to be 300 kJ mol^{-1}, while that for reaction (5) was assumed to depend linearly on the surface coverage, θ, according to $375-154\theta$ kJ mol^{-1}.

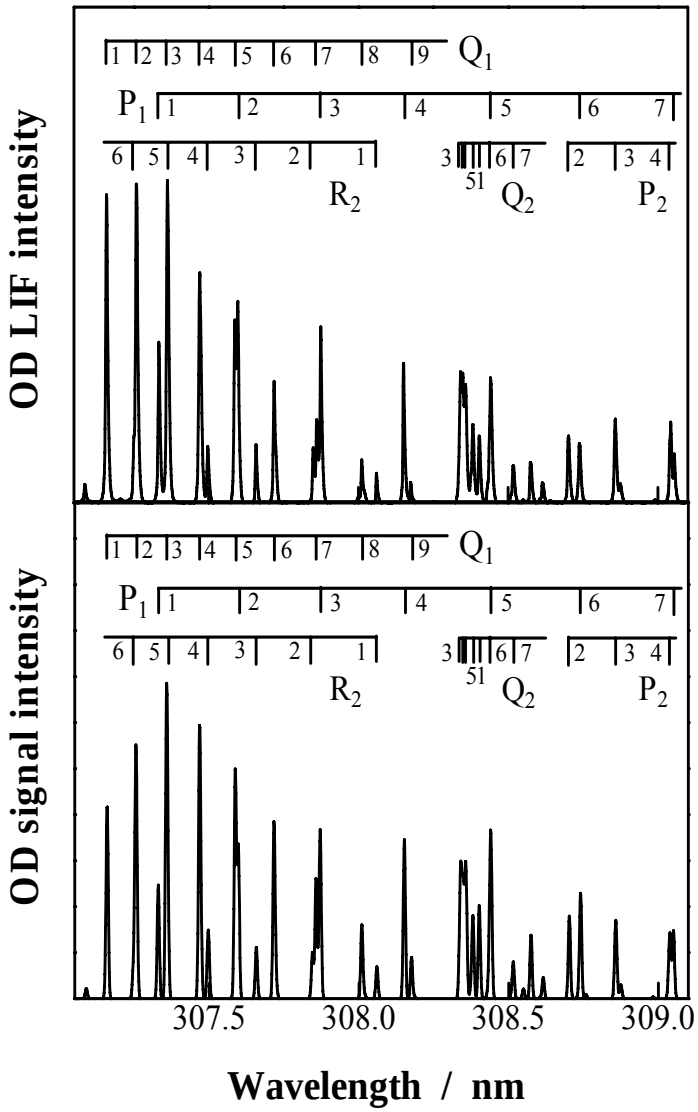
OD LIF intensity
OD signal intensity
1 2 3 4 5 6 7 8 9 Q1
P1 1 2 3 4 5 6 7
6 5 4 3 2 1 R2
3 51 6 7 Q2
2 3 4 P2
307.5
308.0
308.5
309.0
Wavelength / nm

Fig. (1).

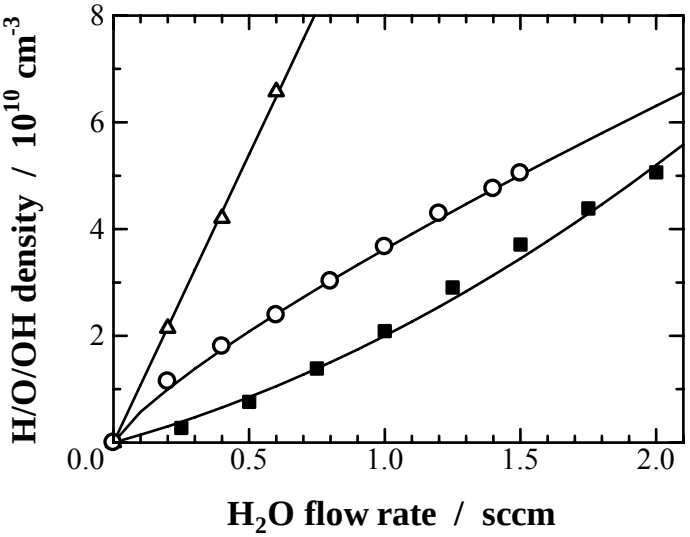

Fig. (2).

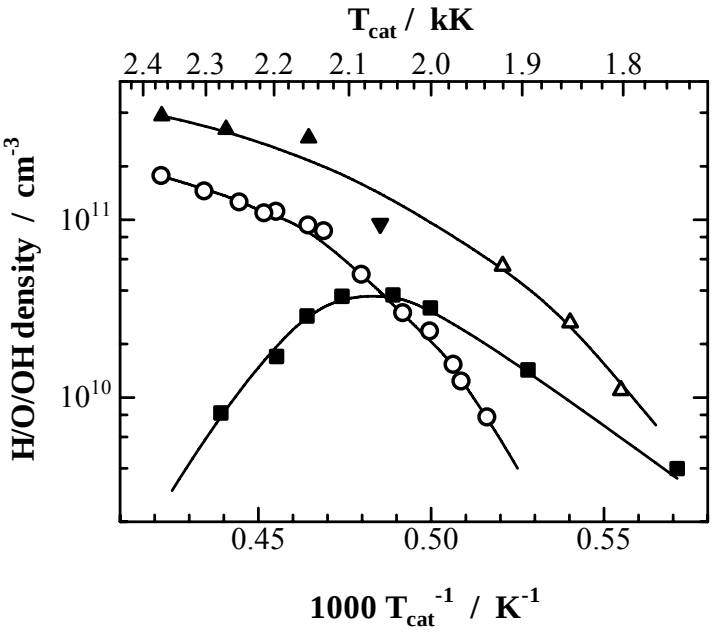
T_cat / kK
2.4 2.3 2.2 2.1 2.0 1.9 1.8
H/O/OH density / cm^-3
10^11
10^10
0.45 0.50 0.55
1000 T_cat^-1 / K^-1

Fig. (3).

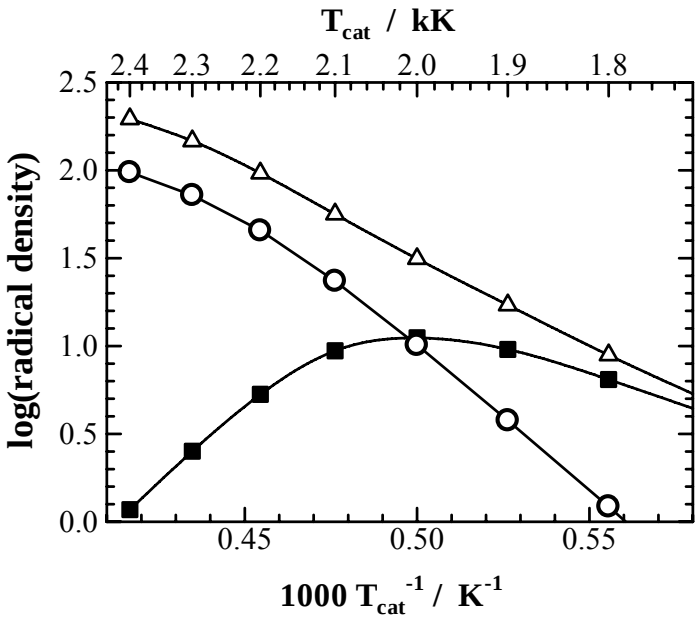
T_cat / kK
2.4 2.3 2.2 2.1 2.0 1.9 1.8
2.5
2.0
1.5
1.0
0.5
0.0
log(radical density)
0.45 0.50 0.55
1000 T_cat^-1 / K^-1

Fig. (4).